This article has been accepted for publication in a future issue of this journal, but has not been fully edited. Content may change prior to final publication. Citation information: DOI 10.1109/TWC.2018.2796553, IEEE Transactions on Wireless Communications

Asynchronous Device Detection for Cognitive Device-to-Device Communications

Bin Li, *Member, IEEE*, Weisi Guo, *Senior Member, IEEE*, Ying-Chang Liang, *Fellow, IEEE*, Chunyan An, Chenglin Zhao

***Abstract*—Dynamic spectrum sharing will facilitate the interference coordination in device-to-device (D2D) communications. In the absence of network level coordination, the timing synchronization among D2D users will be unavailable, leading to inaccurate channel state estimation and device detection, especially in time-varying fading environments. In this study, we design an *asynchronous* device detection/discovery framework for cognitive-D2D applications, which acquires timing drifts and dynamical fading channels when directly detecting the existence of a proximity D2D device (e.g. or primary user). To model and analyze this, a new dynamical system model is established, where the unknown timing deviation follows a random process, while the fading channel is governed by a discrete state Markov chain. To cope with the mixed estimation and detection (MED) problem, a novel sequential estimation scheme is proposed, using the conceptions of statistic Bayesian inference and random finite set. By tracking the unknown states (i.e. varying time deviations and fading gains) and suppressing the link uncertainty, the proposed scheme can effectively enhance the detection performance. The general framework, as a complimentary to a network-aided case with the coordinated signaling, provides the foundation for development of flexible D2D communications along with proximity-based spectrum sharing.**

***Index Terms*—D2D, spectrum sharing, out-of-coverage, device discovery/detection, asynchronous detection, Bayesian inference**

I. Introduction

DEVICE to device (D2D) communications, which exploit the natural proximity of randomly distributed devices and establish a direct link between two neighbors without routing via based-station (BS) [1]–[3], constitute an appealing way to flexibly deploy future wireless networks. By offering the prospect of improved resource utilization (i.e. both the spectrum and energy efficiency), D2D may also effectively alleviate the bottleneck effect of BS and thereby promotes the overall throughput of cellular networks [4], [5]. In this regards, D2D has the potential to accommodate for the expected explosion in the number of wireless devices (e.g. 10× increasing in 2019) [6], and forms part of the envisaged 5G ultra-dense networks [7], [8].

Bin Li and Chenglin Zhao are with the School of Information and Communication Engineering (SICE), Beijing University of Posts and Telecommunications (BUPT), Beijing, 100876, China (Email: stonebupt@gmail.com). Weisi Guo is with School of Engineering, University of Warwick, West Midlands, CV47AL (Email: Weisi.Guo@warwick.ac.uk). Y.-C. Liang is with University of Electronic Science and Technology of China (UESTC), Chengdu 611731, China (e-mail: liangyc@ieee.org). Chunyan An is with State Grid Corporation of China (SGCC), Global Energy Internet Research Institute (GEIRI), Beijing, 102209, China (Email: anchunyan@sgri.sgcc.com.cn). This work was supported in part by Natural Science Foundation of China (NSFC) under Grants 61471061, 61571100 and 61631005.

In D2D, despite the benefits of centralized coordination from BS [9]–[11], minimal involvement of network will be of critical importance, especially in fallback publicity safety scenarios or out-of-coverage applications [2], [12], [13]. In adverse situations (e.g. without dedicated pilot or timing synchronization), D2D devices have to probe the surrounding and adjust their transmission strategies to control interference, using its own distributed sensing of unknown environments. As a complementary to network-aided D2D communications, the interference coordination will be expected to be realized intelligently by D2D devices themselves.

Focusing on the non-coordinated and asynchronous scenarios, the combination of dynamic spectrum sharing (DSS) and D2D, known as cognitive D2D (C-D2D), is considered in this paper, and a potential paradigm for future D2D communications is studied. The major advantages of C-D2D are two-fold. First, the spectrum scarcity, worsened by the emerging ultra-dense networks, will be alleviated by opportunistically accessing spectrum in proximity [14], [15]. Recently, LTE in unlicensed band (LTE-U) opens a wide perspective for DSS-based commercial communications. Second, a listen-before-talk (LBT) technique provides a natural tool of interference mitigation, by excluding the coordination from BS. Thus, the listening to unknown wireless environments, e.g. detecting or discovering active device, will be of great importance to C-D2D [11], [16], [17]. Note that, in the context of C-D2D, the device discovery and spectrum detection may have the same formulation, i.e. directly identifying whether there are signals on the specific band and, if possible, estimating what the associated link information states (LSI) are, see Fig. 1-a. For asynchronous C-D2D communications, direct device discovery/detection [18], which will be implemented in a *blind* manner [19], thereby requires in essence two functions: the existence detection and the LSI acquisition.

The *first* objective, i.e. identifying active user on specific spectrum, can be solved by classical spectrum sensing methods [16], [21], for examples, energy detector [22] or other schemes [17], e.g. the covariance-based technique [23] and the compressive sensing [20], if there exists no information uncertainty. In non-coordinated scenarios, unfortunately, traditional detection algorithms will become less attractive. For one thing, the accurate timing of detection tends to be infeasible. I.e., there is no agreement among unassociated devices and, therefore, random timing drifts between emission and detection slots are inevitable. As a result of such an information uncertainty, the involved statistics in detection, i.e. the summed energy or the instantaneous signal-to-noise ratio (SNR), would

This article has been accepted for publication in a future issue of this journal, but has not been fully edited. Content may change prior to final publication. Citation information: DOI 10.1109/TWC.2018.2796553, IEEE Transactions on Wireless Communications

be unknown. So, it is unable to determine a proper decision threshold for detection. For another, the wireless environment may also change dynamically [24], [25], which renders the fading channel time-dependent and arouses additional information uncertainty in decision process, further deteriorating the detection performance. Whilst the fixed-threshold technique may be used (e.g. relying on a Neyman-Pearson criterion), it would noticeably degrade the performance, by causing the high miss detection (as illustrated by Fig. 1-b) and thereby the harmful interferences to primary transmission. Another expedient approach is to marginalize such uncertain states (e.g. dynamical channel or timing drift) [22] or exploiting their expectation as one practical alternative, which achieves less competitive performance.

The *second* objective, the acquisition of LSI will be of great significance to C-D2D communications [26], which should be estimated in real-time, in order to improve detection performance and optimize subsequent transmission. For example, except for promoting device detection, accurate timing is required in the hand-shake of two devices in proximity, whilst channel gains are critical to power control and mode selection (if the network involvement is available) [11], [32]. However, in out-of-coverage situations the acquisition of such LSI must be realized blindly, at the same time of detecting unassociated device. The involved two-level interruptions, i.e. (1) the mutual influence in estimating unknown timing and channel gains, and (2) the mutual interruption between detection and estimation as well as the resulting error propagation, will make most Bayesian schemes invalid.

In this study, a novel asynchronous device detection paradigm is proposed for C-D2D communications, whereby the centralised coordination tend to be not practical. To be specific, we formulated the challenging task as one track-before-detect (TBD) problem, as known in the target-tracking literature [27]–[29]. In contrast to conventional sensing approaches where the signal is first detected, and then the signal is estimated, our new scheme jointly accomplishes detection and estimation in order to make use of all statistic information available in received signals. To do so, rather than a classical two-hypothesis test (THT) formulation, we adopted another new concept of random finite set (RFS). By unifying the binary existence of target signals and the associated state of object as one generalized random variable, RFS has become one powerful analysis tool to deal with object tracking problems [25], [26], [28], [30], [31], [43]. To sum up, the main contributions are summarized as follows.

1. We consider two inherent difficulties in C-D2D device detection, and thereby formulate a general dynamical system model. Both evolving timing drifts and time-dependent fading channels are cast into the model. Such two information uncertainties, which are characterized respectively by two random processes, are viewed as two hidden states to be estimated.

2. We find multiple *heterogeneous* random variables render the algorithm design a tough work. Specifically, the device detection concerns an unknown binary variable (i.e. "1" for active or "0" for sleep), whilst the estimation of timing drifts and fading channels is associated with another high-dimensional discrete space. Meanwhile, the timing drift is input-dependent, while the channel fading is input-independent. Another major challenge is that the detection and estimation process will be coupled mutually. To combat this, we treat the mixed detection and estimation (MDE) process as one generalized estimation problem, and formulate the heterogeneous variables as one Bernoulli RFS.

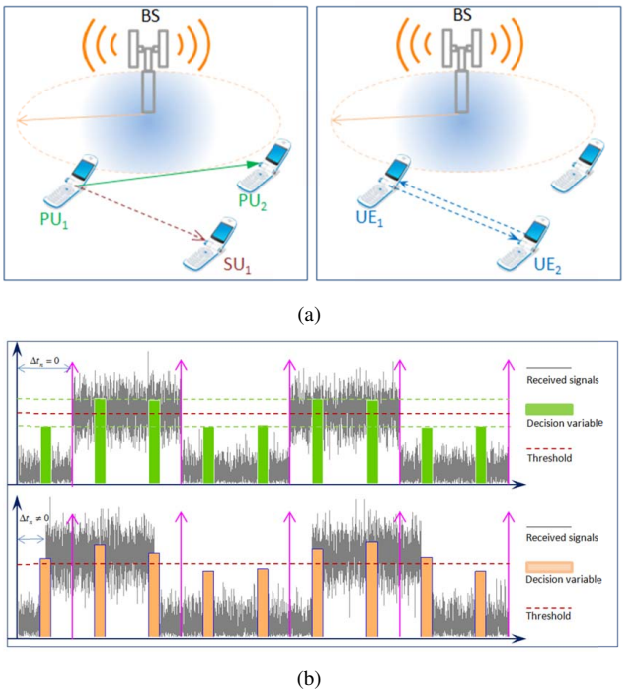

Fig. 1. (a) *Left*: The spectrum detection is performed by a secondary user, while the two primary users are communicating with each other. *Right*: The device discovery is realized among two UEs. (b) *Top*: The synchronization between the unassociated device and the D2D devices is accomplished. *Bottom*: The dynamic timing drift exists among two unassociated devices.

3. We propose a flexible algorithm relying on Bayesian statistical inference, which accomplishes the devices detection (or spectrum sensing) and, at the same time, acquires two dynamical LSI. To address the MDE problem, which is probably beyond the capacity of classical estimation techniques, the designed scheme is based essentially on a sequential maximum *a posteriori* (MAP) criterion. Simplified implementation of the recursive estimation is then investigated, by resorting to a sequential importance sampling (SIS) technique.

4. We evaluate the detection/estimation performance in the presence of dynamical timing drift and time-dependent fading channel. It is demonstrated via simulation that, using our new algorithm, both two unknown LSI will be tracked accurately. The information uncertainty, therefore, can be reduced to the maximum, and the detection performance will be promoted. By alleviating the inflexible requirement on coordinated timing or pilot signaling, the proposed scheme will show the great promise to future C-D2D communications, by facilitating the spectrum-efficient and proximity-inspired transmissions.

The rest of the work is structured as following. In Section II, a general system model is formulated in the context of time drifts and non-stationary channel fading. Subsequently, a Bayesian sequential estimation, relying on RFS, is briefly introduced in Section III. Then, a new scheme which jointly

This article has been accepted for publication in a future issue of this journal, but has not been fully edited. Content may change prior to final publication. Citation information: DOI 10.1109/TWC.2018.2796553, IEEE Transactions on Wireless Communications

estimates time-varying LSI and device state is proposed, by presenting a flexible Bernoulli filtering scheme. In Section IV, numerical results and performance analysis are provided. Finally, we conclude this investigation in Section V.

II. System Model

In this paper, we consider a distributed D2D communication network, which employs dynamic spectrum access. The main motivations will be two aspects. First, a cluster-header is usually resource-demanding and becomes the network bottleneck in terms of energy and longevity [2], [33]. Second, a centralized control relies on frequent information exchanges, which becomes even impractical in adverse environments.

In C-D2D, the device discovery, or spectrum sensing, share the same problem formulation, as illustrated in Fig. 1-(a). For *spectrum sensing*, a PU device will occupy a frequency band, while the SU manages to identify whether this band is occupied and utilizes a DSS strategy to avoid interference. If the band is unoccupied, a SU will access and talk with another proximity device; otherwise, it will sense another band [21], [24]. For direct *device detection*, a UE will sense the specific channel to find one potential device in proximity for data transmission. This process is also blind, in the case of out-of-coverage D2D scenario, as in spectrum sensing. More importantly, except for the similar objective, the unknown LSI involved in above two processes are almost the same.

(1) Due to the lack of centralized coordination, the timing information among two unassociated devices will be unavailable. To this end, as illustrated in Fig. 1-(b), a detection slot may be deviated from the emission slot of another device. Thus, the statistical likelihood of decision variable will become unknown and the detection performance will be deteriorated remarkably, as a decision threshold is associated with with varying timing drifts.

(2) Meanwhile, given dynamical wireless environments (e.g. aroused by device mobility), the channel gain for a particular frequency will be time-dependent, by introducing random fluctuations in received signals. Combined with the timing drifts, the resulting serious information uncertainty poses formidable challenges to accurate device detection/discovery in asynchronous C-D2D scenarios.

A. Dynamic State-Space Model

For the device detection in C-D2D communications, a new dynamical system model is established, i.e.,

$$s_n = S(s_{n-1}), \tag{1}$$

$$M_n = T(M_{n-1}, u_n), \tag{2}$$

$$\alpha_n = H(\alpha_{n-1}), \tag{3}$$

$$z_n = Z(t_n, \alpha_n, s_n, \{w_{n,m}\}_{m=1}^{M}). \tag{4}$$

Here, Eqs. (1)-(3) are referred as to *dynamic* equations, which respectively describe the stochastic transitions (from discrete time $n-1$ to time n) of unknown states, i.e., the existence state s_n, the discrete timing drift M_n and the fading gain α_n. Eq. (4) is the *measurement* equation, which specifies the coupling relationship between unknown states (M_n,α_n) and the observation z_n at time n.

B. Dynamics of PU States

The first stochastic function $S(\cdot) : \mathbb{Z}^1 \mapsto \mathbb{Z}^1$ specifies the dynamical behavior of device states at the nth time. To be specific, s_n=1 indicates the existence of an active device, while s_n=0 represents the absence of active device. Here, it is modeled as one 1st-order Markov process, i.e. $s_n \in \mathcal{S} \triangleq \{0, 1\}$ [34], [35]. Accordingly, its transitional probability matrix (TPM) is given by:

$$\mathbf{P} = \begin{bmatrix} 1-p_b & p_b \\ 1-p_s & p_s \end{bmatrix}, \tag{5}$$

where p_s denotes the survival probability, i.e., the probability of a PU stays in an active state S_1 and also in S_1 at the previous slot and the current slot, i.e., $p_s := \Pr\{s_{n+1} = 1 | s_n = 1\}$. p_b is the birth probability, i.e., the probability a PU keeps inactive state in S_0 at the previous slot and switches to S_1 at the current slot n, $p_b := \Pr\{s_{n+1} = 1 | s_n = 0\}$.

Given the prior TPM, the inexplicit dynamic function $S(s_{n-1})$ will be determined via:

$$\Pr\{S(s_{n-1}) = s_n\} = \Pr\{s_{n-1} | s_n\}, s_n \in \mathcal{S}. \tag{6}$$

C. Dynamics of Channel Fading

The dynamical function $H(\cdot) : \mathbb{R}^1 \mapsto \mathbb{R}^1$ characterizes the transition of channel fading $\alpha_n \in \mathcal{A}$ ($\mathcal{A} \subset \mathbb{R}^1$). Note that, here we focus on the fading gain (as required by the non-coherent observation and the mode selection application when roughly evaluating SNRs), which is modeled as one discrete-state Markov chain (DSMC) [36]–[38]. Different from the other auto-regressive (AR) model, the stochastic dynamic function $H(\alpha_{n-1})$ will be determined by a group of transitional probabilities, i.e.,

$$\Pr\{H(\alpha_{n-1}) = \alpha_n\} = \Pi_{k \to k'}, \quad \alpha_{n-1}, \alpha_n \in \mathcal{A}.$$

Here, each transitional term $\Pi_{k \to k'}$ defines the probability of a fading state α_n, switching from the state k at time index $(n'-1)$ to the state k' at time index n', i.e.,

$$\Pi_{k \to k'} \triangleq \Pr\left(\alpha_{n'} = \mathsf{A}_{k'} | \alpha_{n'-1} = \mathsf{A}_k\right). \tag{7}$$

For the slowly evolving fading, the transitional time is denoted as $n' = \lfloor n/L \rfloor$ [24], [36], where L is the static length in which the fading gain α_n will remain unchanged temporarily. Taking the Rayleigh fading of $|\mathcal{A}| = K$ states for example, i.e. $f(\alpha_n) = \frac{\alpha_n}{\sigma_\alpha^2} \times \exp(-\frac{\alpha_n^2}{2\sigma_\alpha^2})$, $\Pi_{i \to j}$ will be derived via:

$$\begin{aligned} \Pi_{k \to k'} &\triangleq \Pr\left(\{\alpha_{n'} \in [v_{k'}, v_{k'+1}) | \alpha_{n'} \in [v_k, v_{k+1})\}\right), \\ &= \frac{1}{\pi_k} \int_{v_{k'}}^{v_{k'+1}} \int_{v_k}^{v_{k+1}} f(\alpha_{n'-1}, \alpha_{n'}) d\alpha_{n'-1} d\alpha_{n'}, \end{aligned} \tag{8}$$

where $f(\alpha_{n'-1}, \alpha_{n'})$ is the bivariate Rayleigh joint probability density function (PDF) [39], and $0 \le k, k' \le |\mathcal{A}| - 1$. The partitioning bounds v_k will divide channel gain into K non-overlapped regions. Using an equiprobable partition rule, i.e. with K equivalent steady probabilities $\pi_k = \int_{v_k}^{v_{k+1}} f(\alpha_n) d\alpha_n = 1/K$, we have $v_k = \left[-2\sigma_\alpha^2 \times \ln(1 - k/K)\right]^{1/2}$, and $\mathsf{A}_k = \int_{v_k}^{v_{k+1}} \alpha_n \cdot$

This article has been accepted for publication in a future issue of this journal, but has not been fully edited. Content may change prior to final publication. Citation information: DOI 10.1109/TWC.2018.2796553, IEEE Transactions on Wireless Communications

$f(\alpha_n)d\alpha_n$ [36], [37]. Here, the first-order DSMC is used, which is sufficient to characterize slow-varying fading channels [24], [36]. Thus, the fading states are related only with its immediate neighborhood states, i.e. $\Theta_{k\to k'}=0$ for $|k-k'|>1$. Accordingly, the TPM of fading channels, denoted by $\mathbf{\Pi}_{K\times K}=\{\Pi_{k\to k'}\},\ k,k'\in\{0,1,\cdots,K-1\}$, is expressed as Eq. (9).

D. Dynamic of timing deviations

We consider two different types of timing drifts.

(1) **Case 1: Uncorrelated drifting** In the first case, the transmission interval of different slots is independent of each other, i.e., $\mathbb{E}\{(t_n-t_{n-1})\cdot(t_{n-1}-t_{n-2})\}=0$. Given the detection slot T_f and the sampling frequency f_s, there contain $M=\lfloor T_f/f_s\rfloor$ samples in each slot. As far as discrete samples are concerned, the deviated samples M_n aroused by timing drifts will be ranged in $\mathcal{M}\triangleq[0,M-1]$, and accordingly, in each slot there contains only $(M-M_n)$ informative samples.

In order to determine the statistical distribution of M_n, assume the interval between two transmissions follow the identically and independently (i.i.d) exponential distribution $\mathscr{E}(\lambda)$, i.e. $\Pr\{t_n-t_{n-1}\}\sim\lambda\cdot\exp\{-\lambda(t_n-t_{n-1})\}$. Given the initial condition t_0=0 and each emission interval $V(n)\triangleq t_n-t_{n-1}$, the nth transmission time will be $t_n=\sum_{l=1}^{n}V(l)$, and the resulting deviation $t_\Delta(n)$ is:

$$t_\Delta(n)=\mathtt{mod}\left[\sum_{l=1}^{n}V(l),T_f\right]\in(0,T_f], \tag{10}$$

where $\mathtt{mod}\,[a,b]$ gives the modulo operation on a with regards to b. For the discrete samples, a similar relation holds, i.e.,

$$M_n=\mathtt{mod}\left[\sum_{l=1}^{n}V_\Delta(l),M\right]\in\mathcal{M}, \tag{11a}$$

$$V_\Delta(n)=\lfloor(t_n-t_{n-1})/T_f\rfloor, \tag{11b}$$

and the i.i.d random variable $V_\Delta(n)$ is also exponentially distributed, i.e. $V_\Delta(n)\sim\mathcal{E}(\lambda_\Delta)$, with $\lambda_\Delta=\lfloor\lambda/T_f\rfloor$. Moving on, we obtain the following equivalent relation, i.e.,

$$\begin{aligned}M_n&=\mathtt{mod}\left\{\sum_{l=1}^{n}\mathtt{mod}\left[V_\Delta(l),M\right],M\right\},\\&=\mathtt{mod}\left[\sum_{l=1}^{n}Y_l,M\right],\quad Y_l\in\mathcal{M}.\end{aligned} \tag{12}$$

It is noted that $Y_l\triangleq\mathtt{mod}\,[V_\Delta(l),M]$ is also an i.i.d random variable, with a discrete PDF specified by a group of probability mass $\{w_m\}$ $(m\in\mathcal{M})$, i.e.,

$$p(Y_n)=\sum_{m=0}^{M-1}w_m\times\delta(Y_n-m), \tag{13}$$

$$w_m=\sum_{k=0}^{\infty}\lambda_\Delta\times\exp[-\lambda_\Delta(m+kM)]. \tag{14}$$

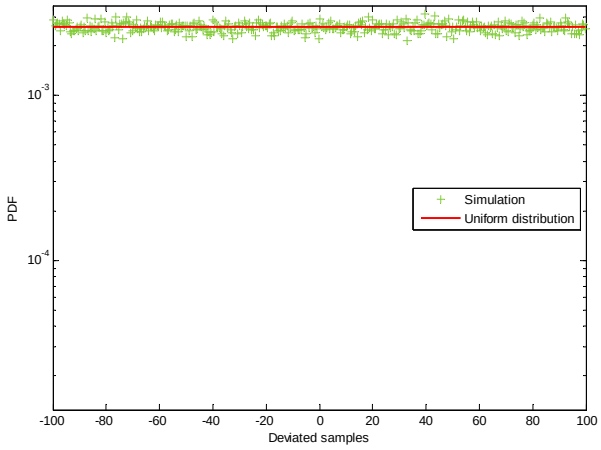

Fig. 2. The distribution of random timing deviations in the case of uncorrelated emission intervals. Each transmission interval is i.i.d distributed according to the negative exponential density of $\lambda_d=10$. The sample length is $M=200$.

For the above modulo operation, the central limits theorem (CLT) for **modulo 1** will be directly applied [40]. I.e., for the i.i.d variable $Y_n\in[0,M-1]$ the modulo on the summation of Y_n will converge weakly to a *uniform* distribution, i.e.,

$$\mathtt{mod}\left[\sum_{l=1}^{n}Y_l,M\right]\overset{n\to\infty}{\longrightarrow}\mathscr{U}(0,M), \tag{15}$$

subject to the condition

$$\lim_{n\to\infty}p(Y_1)p(Y_2)\cdots p(Y_n)=0.$$

We then show that, for the above considered case, the term $\Delta_n\triangleq p(Y_1)p(Y_2)\cdots p(Y_n)$ satisfies

$$\begin{aligned}\Delta_n&=\prod_{l=0}^{n}\sum_{m=1}^{M-1}\sum_{k=1}^{\infty}\lambda_\Delta\times\exp\{-\lambda_\Delta[m+kM]\},\\&<\prod_{l=0}^{n}\sum_{m=1}^{M-1}\lambda_\Delta\times\exp\{-\lambda_\Delta\cdot m\},\\&<\prod_{l=0}^{n}\lambda_\Delta\times\exp\{-\lambda_\Delta\}=\lambda_\Delta^n\times\exp(-n\lambda_\Delta)\overset{n\to\infty}{\longrightarrow}0.\end{aligned}$$

Thus, relying on the modulo-CLT, the deviated samples M_n in uncorrelated cases will be distributed according to $\mathscr{U}(0,M)$, as further verified by Fig. 2. So, the transitional function $T(t_{n-1})$ will be given as:

$$\Pr\{T(t_{n-1}|t_{n-1})\}=\Pr\{T(t_{n-1})\}=1/M. \tag{16}$$

(2) **Case 2: Correlated drifting** With correlated transmission intervals, the emission interval of the nth time will become correlated with the previous $(n-1)$th slot, i.e.

$$\mathbf{\Pi}_{K\times K}=\begin{bmatrix}\Pi_{0\to0}&\Pi_{0\to1}&0&0&\cdots&0&0&0\\\Pi_{1\to0}&\Pi_{1\to1}&\Pi_{1\to2}&0\cdots&0&0&0&\\\vdots&\vdots&\vdots&\vdots&\ddots&\vdots&\vdots&\vdots\\0&0&0&0&\cdots&\Pi_{(K-2)\to(K-3)}&\Pi_{(K-2)\to(K-2)}&\Pi_{(K-2)\to(K-1)}\\0&0&0&0&\cdots&0&\Pi_{(K-1)\to(K-2)}&\Pi_{(K-1)\to(K-1)}\end{bmatrix}. \tag{9}$$

This article has been accepted for publication in a future issue of this journal, but has not been fully edited. Content may change prior to final publication. Citation information: DOI 10.1109/TWC.2018.2796553, IEEE Transactions on Wireless Communications

$\mathbb{E}\{(t_n - t_{n-1})(t_{n-1} - t_{n-2})\} \neq 0$. In this case, the statistical distribution of timing drifts will be hardly derived, and alternatively, we use a general Gaussian model to describe the stochastic procedure, i.e.,

$$t_n = t_{n-1} + \tau_n,$$

where the driven term τ_n is assumed to follow an i.i.d Gaussian process [41], with the zero mean and the variance σ_τ^2. It is found that, for the discrete samples, the samples deviation M_n will be characterized by:

$$M_n = M_{n-1} + \Delta_n, \tag{17}$$

where the discrete driven term Δ_n accordingly follows a discrete Gaussian process $\mathscr{N}_d(0, \sigma_\Delta^2)$.

It should be notworthy that, as far as the real timing t_n is concerned, the resulting deviation M_n will be always positive. For the convenience of analysis, yet we will consider the discrete deviation M_n is equivalently ranged in $[-M/2, M/2]$. That is, a negative M_n accounts for the advanced drift, i.e., the M_n deviated samples fall into the previous $(n-1)$th slot; whilst a positive M_n indicates the delayed drifting and M_n samples fall to the next $(n+1)$th slot. Of course, the other equivalent formulation $M_n \in [-M, M]$ can be also applicable, and the designed algorithm is independent of specific prior information. As such, we have:

$$\begin{aligned}&\Pr\{M_n|M_{n-1}\} \qquad (18)\\ &= \begin{cases} 1\Big/\sqrt{2\pi\sigma_\Delta^2}\cdot\exp[-(M_n - M_{n-1})^2/2\sigma_\Delta^2], & \text{case 1},\\ \mathscr{U}(-M/2, M/2], & \text{case 2}.\end{cases}\end{aligned}$$

E. Observation

The observation $z_n \in \mathcal{Z}(\mathcal{Z} \subset \mathbb{R}^1)$ at the nth detection slot will be calculated via:

$$\begin{aligned}z_n &= \sum_{m=1}^{M}\Big\{\alpha_n c_n(m)\delta(s_n - 1)G_{M_n}(m) + w_n(m)\Big\}^2, \qquad (19)\\ &= \begin{cases}\displaystyle\sum_{m=1}^{M}\Big\{\alpha_n c_n(m)G_{M_n}(m) + w_n(m)\Big\}^2, & s_n = 1,\\ \displaystyle\sum_{m=1}^{M} w_n^2(m), & s_n = 0.\end{cases}\end{aligned}$$

Here, $\delta(x)$ denotes a Dirichlet function, which indicates the existence of the target signal; $G_{M_n}(m)$ $(m = 1, 2, \cdots, M)$ accounts for a window function imposed on target signals, which is aroused by timing drifts M_n. H_0 and H_1 correspond to two hypotheses, respectively, i.e., the absence and presence of target signals $c_n(m) = b_n(m) \times p(m)$, where $b_n(m)$ represent the unknown information symbols, and $p(m)$ is the pulse-shaping response. For simplicity, the binary phase shift keying (BPSK) signal is considered, i.e. $b_n(m) \in \mathcal{B} = \{\sqrt{E_s}, -\sqrt{E_s}\}$ with $\mathbb{E}_{\mathcal{B}}\{b_n^2(m)\} = E_s$. The noise samples $w_n(m) \in \mathbb{R}^1$ are assumed to be zero-mean additive white Gaussian noise (AWGN) which is independent of other hidden states, i.e., $w_n(m) \sim \mathscr{N}(0, \sigma_w^2)$. When the non-coherent observations are concerned [24], [25], the generalization of the model and subsequent algorithm to other unknown modulated signals will be straightforward.

Note that, when M_n=0 we have $G_{M_n}(m) = 1$ for $m = 1, \cdots, M$. For the positive $M_n > 0$, the window function $G_{M_n}(m)$ will be specified by:

$$G_{M_n}(m) = \begin{cases} 0, & 1 \leq m \leq M_n, \qquad (20a)\\ 1, & M_n + 1 \leqslant m \leq M, \qquad (20b)\end{cases}$$

and for a negative $M_n < 0$, we have

$$G_{M_n}(m) = \begin{cases} 1, & 1 \leq m \leq M - |M_n|, \qquad (21a)\\ 0, & M - |M_n| + 1 \leq m \leq M. \qquad (21b)\end{cases}$$

Considering a case $M_n > 0$, two pieces of summed energy will be calculated respectively, i.e.,

$$z_n(1) = \sum_{m=1}^{M_n} w_n^2(m),\ z_n(2) = \sum_{m=M_n+1}^{M}[\alpha_n c_n(m) + w_n(m)]^2.$$

It is found that such two components will be independent of each other. Given independent noise samples, the likelihood function $p\{z_n|\alpha_n, s_n = 1, M_n\}$ is evaluated via $p\{z_n(1)|s_n = 1, M_n\} \times p\{z_n(2)|\alpha_n, s_n = 1, M_n\}$. Here, $p\{z_n(1)|s_n = 1, M_n\}$ follows the central Chi-square distribution of the degree M_n, while $p\{z_n(2)|\alpha_n, s_n = 1, M_n\}$ follows a non-central Chi-square density of the degree $(M - M_n)$ with a non-central parameter $[M - M_n] \cdot \mathbb{E}\{c_n^2(m)\}\alpha_n^2/\sigma_w^2$.

When both $M - M_n$ and M_n are sufficiently large (>20), then each component ($z_n(1)$ or $z_n(2)$) follows the Gaussian distributions, according to the CLT. Given different emission status of unassociated devices (i.e. s_n) as well as the related LSI (i.e., α_n and M_n), the approximated likelihood distributions will be:

$$\varphi_n(z_n|s_n = 0) = \mathscr{N}\{M\sigma_w^2, 4M\sigma_w^4\}, \tag{22}$$

$$\begin{aligned}&\varphi_n(z_n|\alpha_n, s_n = 1, M_n) =\\ &\quad\mathscr{N}\{\mathbb{E}\{z_n(1)|s_n = 1, M_n\}, \mathbb{V}\{z_n(1)|s_n = 1, M_n\}\} \times\\ &\quad\mathscr{N}\{\mathbb{E}\{z_n(2)|s_n = 1, M_n\}, \mathbb{V}\{z_n(2)|s_n = 1, M_n\}\}. \qquad (23)\end{aligned}$$

where each single mean and variance terms, in the case of s_n=1, will be given by:

$$\begin{aligned}&\mathbb{E}\{z_n(1)|s_n = 1, M_n > 0\} = M_n\sigma_w^2,\\ &\mathbb{V}\{z_n(1)|s_n = 1, M_n > 0\} = 4M_n\sigma_w^4,\\ &\mathbb{E}\{z_n(2)|\alpha_n, s_n = 1, M_n > 0\} = 2(M - M_n)E_s\alpha_n^2\sigma_w^2,\\ &\mathbb{V}\{z_n(2)|\alpha_n, s_n = 1, M_n > 0\} = 2(M - M_n)E_s\alpha_n^2\sigma_w^2\\ &\qquad\qquad + 4(M - M_n)\sigma_w^4.\end{aligned}$$

III. Asynchronous Device Detection

To implement the mixed device detection and LSI estimation in the context of unknown timing, we adopt the maximum *a posteriori* (MAP) criterion and design a stochastic filtering scheme. Rather than relying on a fixed threshold, we manage to exploiting fully the dynamical statistics involved in the received signals. Our new scheme is thereby rooted on a Bayesian rule, which is committed to estimate the joint posterior density, i.e.,

$$(\hat{\alpha}_n, \hat{s}_n, \hat{M}_n) = \arg\max_{\alpha_n \in \mathcal{A}, s_n \in \mathcal{S}, M_n \in \mathcal{M}} p(\alpha_{1:n}, s_{1:n}, M_{1:n}|z_{1:n}), \tag{24}$$

This article has been accepted for publication in a future issue of this journal, but has not been fully edited. Content may change prior to final publication. Citation information: DOI 10.1109/TWC.2018.2796553, IEEE Transactions on Wireless Communications

where $s_{1:n} = \{s_1, s_2, \cdots, s_n\}$ denotes the trajectory of transmission states until the nth slot, while $\alpha_{1:n}$, $M_{1:n}$ and $z_{1:n}$ are three trajectories of fading gains, varying timing drifts and observations, respectively. It is noteworthy that, relying on a concept of THT, the Neyman-Pearson (NP) criterion becomes inadequate to the new formulation of joint estimation [35].

A basic idea here is the recursive estimation, which exploits the underlying dynamics of unknown states. That means, a sequential Bayesian framework, i.e., predict using the Chapman-Kolmogorov (CK) equation and then updating with the Bayesian rule, will be adopted. A major difficulty is that, unlike the tracking of an established link channel, the likelihood density will be *unavailable* due to the random presence/absence of device. Therefore, the formulated MDE problem in Eq. (24) still remains a substantial challenge.

In the section, we suggest a new formulation to characterize the stochastic presence of device and the dynamics of its related LSI (i.e. the varying timing drift and channel fading). Then, for the specific application we further design a sequential estimation scheme.

A. Random Finite Set

We formulate a Bernoulli RFS (BRFS) $\boldsymbol{\mathcal{F}}_n$ to characterize asynchronous device detection with unknown LSI. To be specific, the BRFS cardinality of time n, which is denoted by $d_n = |\boldsymbol{\mathcal{F}}_n|$ ($d \in \mathbb{N}_0 = \{0, 1, \cdots\}$) and follows a Bernoulli distribution $\kappa(d) = \Pr\{|\boldsymbol{\mathcal{F}}_n| = d\}$ [30], [31], [42], is used to indicate whether an device is transmitting signal or not. Meanwhile, a compound state $\mathbf{f}_n \triangleq \{M_n, \alpha_n\} \in \mathcal{A} \times \mathcal{M} \subset \mathbb{R}^2$, related with an unassociated device, consists of unknown timing drifts and fading gains, which evolves with time. Thus, an RFS $\boldsymbol{\mathcal{F}}_n$ is able to cast two-level uncertainties into one random process, i.e., whether there are target signals and what its related LSI is.

In following analysis, we adopt the Mahler's approach to define the finite set statistics (FISST) PDF of $\boldsymbol{\mathcal{F}}_n$ [30], i.e.,

$$p(\boldsymbol{\mathcal{F}}_n = \{\mathbf{f}_1, \mathbf{f}_2, \cdots, \mathbf{f}_d\}) = n!\kappa(d_n) \cdot p(\{\mathbf{f}_1, \mathbf{f}_2, \cdots, \mathbf{f}_d\}). \quad (25)$$

In the context of the *set integral* operation $\int p(\boldsymbol{\mathcal{F}}_n) d\boldsymbol{\mathcal{F}}_n$ (rather than the distribution integration), $p(\boldsymbol{\mathcal{F}}_n)$ can be viewed as one PDF, i.e., $\int p(\boldsymbol{\mathcal{F}}_n)\delta\boldsymbol{\mathcal{F}}_n = p(\boldsymbol{\mathcal{F}}_n = \varnothing) + [1 - p(\boldsymbol{\mathcal{F}}_n = \varnothing)] \times \int p(\mathbf{f}_n) d\mathbf{f}_n = 1$. For the considered BRFS, i.e., $|\boldsymbol{\mathcal{F}}_n|$=1, the above FISST PDF $p(\boldsymbol{\mathcal{F}}_n)$ is rewritten to:

$$p(\boldsymbol{\mathcal{F}}_n) = \begin{cases} 1 - q_n, & \text{if } \boldsymbol{\mathcal{F}}_n = \varnothing, \quad (26a) \\ q_n \times p(\{M_n, \alpha_n\}), & \text{if } \boldsymbol{\mathcal{F}}_n = \{M_n, \alpha_n\}. \quad (26b) \end{cases}$$

Note that, for the cases $d_n > 1$ we will have $p(\boldsymbol{\mathcal{F}}_n)$=0. In other words, in a Bernoulli RFS an unassociated device is either active (e.g. with a probability of q_n) or inactive (e.g. with a probability of $1 - q_n$) [43]. Accordingly, the cardinality density is specified as:

$$\kappa(d) = \begin{cases} 1 - q_n, & \text{if } \boldsymbol{\mathcal{F}}_n = \varnothing, \quad (27a) \\ q_n, & \text{if } \boldsymbol{\mathcal{F}}_n = \{M_n, \alpha_n\}. \quad (27b) \end{cases}$$

B. Sequential MAP

Using the Bayesian sequential inference, the transitional densities of unknown states as well as the likelihood on new observation will be fully utilized. Thus, a two-stage recursive procedure will be implemented, i.e.

$$p_{n|n-1}(\boldsymbol{\mathcal{F}}_n|y_{1:n-1}) = \int_{\boldsymbol{\mathcal{F}}_{n-1}} \phi_{n|n-1}(\boldsymbol{\mathcal{F}}_n|\boldsymbol{\mathcal{F}}_{n-1}) \times p_{n-1|n-1}(\boldsymbol{\mathcal{F}}_{n-1}|y_{1:n-1}) d\boldsymbol{\mathcal{F}}_{n-1}, \quad (28)$$

$$p_{n|n}(\boldsymbol{\mathcal{F}}_n|y\mathbf{z}_{1:n}) = \frac{\varphi_n(y_n|\boldsymbol{\mathcal{F}}_n) p_{n|n-1}(\boldsymbol{\mathcal{F}}_n|y_{1:n-1})}{\int_{\boldsymbol{\mathcal{F}}_n} \varphi_n(y_n|\boldsymbol{\mathcal{F}}_n) p_{n|n-1}(\boldsymbol{\mathcal{F}}_n|y_{1:n-1}) d\boldsymbol{\mathcal{F}}_n}. \quad (29)$$

As mentioned, the one-step prediction of Eq. (28) mainly utilizes the prior traditional information and a C-K equation [44]. The updating stage in Eq. (29) relies on a Bayesian rule, by fully exploiting the real-time information carried with the new observation. Compared to classical Bayesian estimation methods, notable difference in the RFS inference is that, rather than the distribution integration, the set integral operations (i.e. $\delta\boldsymbol{\mathcal{F}}_n$) will be used.

Recalling the previous Markov models, the transitional density of our formulated BRFS, i.e., $\phi_{n|n-1}(\boldsymbol{\mathcal{F}}_n|\boldsymbol{\mathcal{F}}_{n-1})$, will be characterized by also a 1st-order Markov process. Conditioned on different feasible states at the time n-1, we have:

$$\phi_{n|n-1}(\boldsymbol{\mathcal{F}}_n|\varnothing) = \begin{cases} 1 - p_b, & \text{if } \boldsymbol{\mathcal{F}}_n = \varnothing, \quad (30a) \\ p_b \cdot b_{n|n-1}(\{M_n, \alpha_n\}), & \text{else}, \quad (30b) \end{cases}$$

and

$$\phi_{n|n-1}(\boldsymbol{\mathcal{F}}_n|\mathbf{f}_{n-1}) = \begin{cases} 1 - p_s, & \text{if } \boldsymbol{\mathcal{F}}_n = \varnothing, \quad (31a) \\ p_s \cdot p_{n|n-1}(\mathbf{f}_n|\mathbf{f}_{n-1}), & \text{else}. \quad (31b) \end{cases}$$

Here, the *a priori* density $b_{n|n-1}(\{M_n, \alpha_n\})$ specifies an initial distribution for a singleton state $|\boldsymbol{\mathcal{F}}_n| = 1$, if one unassociated device that does not exist at time n-1 is appeared at the time n, i.e. $b_{n|n-1}(\{M_n, \alpha_n\}) = \Pr\{\{M_n, \alpha_n\}|q_{n-1} = 0\}$, as discussed shortly.

C. Bernoulli Filtering

The above sequential estimation, in the context of random absence of target signals, remain relatively different from classical Bayesian estimation, e.g. the Kalman filtering [37]. In sharp contrast, two coupled posterior densities need to be estimated jointly, in order to determine the FISST PDF $p_{n|n}(\boldsymbol{\mathcal{F}}_n|z_{1:n})$ in Eq. (26). The first one, referred as to the existence density, indicates whether the target signal is contained in received samples, i.e.,

$$q_{n|n} \triangleq \Pr\left(|\boldsymbol{\mathcal{F}}_n| = 1, s_n = 1|z_{1:n}\right), \quad (32)$$

The second one is used to characterize the related LSI (e.g. unknown timing drifts and fading gains) when an unassociated device is active at time n, which is also known as the *a posteriori* spatial PDF, i.e.,

$$p_{n|n}\left(\boldsymbol{\mathcal{F}}_n = \{M_n, \alpha_n\}\right) \triangleq \Pr(\alpha_n = \mathsf{H}_{k,j}, M_n). \quad (33)$$

This article has been accepted for publication in a future issue of this journal, but has not been fully edited. Content may change prior to final publication. Citation information: DOI 10.1109/TWC.2018.2796553, IEEE Transactions on Wireless Communications

Solving the above RFS inference process will be premised on a similar two-stage process. In the first stage, the above two densities will be predicted relying on the prior transitional densities as well as the posterior densities of previous time $n-1$. In the second stage, such two predicted densities will be updated by further exploiting the current observation.

1) Prediction Stage: With the help of C-K equation, the 1st-order prediction process will be realized. Given the posterior density of time $n-1$, i.e. $q_{n-1|n-1}$ and $p_{n-1|n-1}(\mathbf{f}_n)$, two predicted distributions of the time n, i.e., $q_{n|n-1}$ and $p_{n|n-1}(\mathbf{f}_n)$, will be derived respectively from Eqs. (34) and (35): (see the bottom of the next Page):

$$q_{n|n-1} = p_b \times (1 - q_{n-1|n-1}) + p_s \times q_{n-1|n-1}. \tag{34}$$

The similar derivation procedure of two above equations may be found in some previous works [26], [35], [43]. The expressions of such two densities are relatively easy to follow. Each predicated density will be contributed by *two* complimentary terms, i.e., the component from a sustained active device (i.e. which is related with $q_{n-1|n-1}$ and known as the *survival* component), and the other component from the newly birthed device (i.e. which is related with $1 - q_{n-1|n-1}$ and refereed as to the *birth* component).

2) Update Stage: Relying on the new observation z_n, the predicted densities attained by the first-stage will be updated. The updated densities, by incorporating the innovation information, will be more accurate, which are given by Eq. (36) (at the bottom of the page) and

$$p_{n|n}(\{M_n, \alpha_n\}) = \frac{r_n(z_n|\{M_n,\alpha_n\}) \times p_{n|n-1}(\{M_n,\alpha_n\})}{\int_{\mathcal{A},\mathcal{M}} r_n(z_n|\{M_n,\alpha_n\}) \times p_{n|n-1}(\{M_n,\alpha_n\}) d\alpha_n dM_n}, \tag{37}$$

where the likelihood ratio is defined as:

$$r_n(z_n|\{M_n,\alpha_n\}) = \varphi_n(z_n|\alpha_n, s_n=1, M_n)/\varphi_n(z_n|s_n=0). \tag{38}$$

With the derived two posterior densities, the unassociated device will be detected via the MAP criterion, i.e.,

$$\hat{s}_n = \begin{cases} 1, & \text{if } q_{n|n} > \gamma, \quad (39a) \\ 0, & \text{if } q_{n|n} \le \gamma, \quad (39b) \end{cases}$$

where γ will be configured to $1/2$ as in a Bayesian rule. Meanwhile, the unknown LSI will be estimated via:

$$\{\hat{M}_n, \hat{\alpha}_n\} = \arg \max_{M_n \in \mathcal{M}, \alpha_n \in \mathcal{A}} p_{n|n}(\{M_n, \alpha_n\}). \tag{40}$$

3) Related Densities: In the analysis, the prior transitional density of dynamical timing drifts will be determined via Eq. (41), which will be dependent of various emission intervals.

$$\begin{aligned} &p_{n|n-1}(\{\alpha_n, M_n\}|\{\alpha_{n-1}, M_{n-1}\}) \\ &= \Pr(\alpha'_n = \mathsf{A}_{k'}|\alpha_{n'-1} = \mathsf{A}_k) \times \Pr(M_n|M_{n^\dagger}) \qquad (41) \\ &= \begin{cases} \Pi_{k\to k'} \cdot \mathscr{N}(M_n - M_{n^\dagger}; 0, \sigma_\Delta^2), & \text{Type 1}, \\ \Pi_{k\to k'} \cdot \mathscr{U}(M_n - M_{n^\dagger}; [-M/2, M/2]), & \text{Type 2}. \end{cases} \end{aligned}$$

Notice that, $n^\dagger$ denotes the previous time slot of unassociated emission. It is noteworthy that this previous emission slot $n^\dagger$ may be smaller than $n-1$. I.e. such an *emission-dependent* dynamical process will be different from that of fading gain, which is closely related with PU's emission states. In other words, the timing drift M_n is not necessary to estimate in the case of $s_n = 0$ and, in contrast, the fading channel needs to be estimated even if s_n=0. To be specific, if an unassociated device is active at time $n-1$, then the estimated fading state is $\hat{\alpha}_{n-1} = \hat{\alpha}_{n-2}$ in the case of $\mathtt{mod}(n-1, L) > 0$ and $s_{n-1} = 0$; otherwise, it will be estimated via the prior transitional density $\hat{\alpha}_{n-1} = \arg \max_{\alpha_{n-1}\in\mathcal{A}} p(\alpha_{n-1}|\hat{\alpha}_{n-2})$ in the case of $\mathtt{mod}(n-1, L) = 0$ and $s_{n-1} = 0$.

It is seen from the predict-update procedure that the proposed scheme can effectively address the aforementioned likelihood disappearance and the mutual interruption problems. First, the combination of birth and survival components, see Eq. (34) and (35), as the expectation on the corresponding densities, would cope with the influence from the *existence* uncertainty ($s_n = 1$ or $s_n = 0$). Second, the mutual interruption is fully embodied by two coupled densities, i.e., the existence density and the spatial density, which can be now estimated jointly.

As mentioned, the birth density will be of importance to sequential estimation, which should be properly designed. In this work, the birth density is specified as in Eq. (42), given the independent timing drift and channel fading, i.e.,

$$b_{n|n-1}(\{M_n, \alpha_n\}) = b_{n|n-1}(\alpha_n) \times b_{n|n-1}(M_n). \tag{42}$$

For the fading gain, a birth sub-density is assigned as:

$$\begin{aligned} b_{n|n-1}(\alpha_n) &= \Pr\{\alpha_n|s_{n-1}=0\}, \qquad (43) \\ &= \int_{\mathcal{A}} p_{n|n-1}(\alpha_n|\tilde{\alpha}_{n-1}) \cdot b_{n-1}(\tilde{\alpha}_{n-1}) d\tilde{\alpha}_{n-1}, \end{aligned}$$

where the term $\tilde{\alpha}_{n-1}$ is viewed as an intermediate state, which is derived from the estimated fading state of previous time

$$\begin{aligned} p_{n|n-1}(\{M_n,\alpha_n\}) =& \frac{p_b \cdot (1 - q_{n-1|n-1}) \times b_{n|n-1}(M_n,\alpha_n)}{q_{n|n-1}} \\ &+ \frac{p_s \cdot q_{n-1|n-1} \times \int_{\mathcal{A},\mathcal{M}} p_{n|n-1}(\{M_n,\alpha_n\}|\{M_{n-1},\alpha_{n-1}\}) \cdot p_{n-1|n-1}(\{M_n,\alpha_n\}) d\alpha_n dM_n}{q_{n|n-1}}. \end{aligned} \tag{35}$$

$$q_{n|n} = \frac{q_{n|n-1} \times \int_{\mathcal{A},\mathcal{M}} r_n(z_n|\{M_n,\alpha_n\}) \cdot p_{n|n-1}(\{M_n,\alpha_n\}) d\alpha_n dM_n}{1 - q_{n|n-1} + q_{n|n-1} \times \int_{\mathcal{A},\mathcal{M}} r_n(z_n|\{M_n,\alpha_n\}) \cdot p_{n|n-1}(\{M_n,\alpha_n\}) d\alpha_n dM_n}. \tag{36}$$

This article has been accepted for publication in a future issue of this journal, but has not been fully edited. Content may change prior to final publication. Citation information: DOI 10.1109/TWC.2018.2796553, IEEE Transactions on Wireless Communications

$n-1$. Given the estimation state $\hat{\alpha}_{n-1}$, we have:

$$b_{n-1}(\tilde{\alpha}_{n-1}=\mathsf{H}_j)=\begin{cases}1/3, & \hat{\alpha}_{n-1}=\mathsf{H}_i \ \& \ |i-j|\leq 1,\\ 0, & \hat{\alpha}_{n-1}=\mathsf{H}_i \ \& \ |i-j|>1.\end{cases}$$

For the timing drift, its birth sub-density is specified by:

$$\begin{aligned} b_{n|n-1}(M_n)&=\Pr(M_n|z_{1:n-1}),\\ &\simeq p_{n|n-1}(M_n|\hat{M}_{n^\dagger}). \end{aligned} \tag{44}$$

D. Implementations

Although the recursive propagation of posterior densities provides a theoretic framework for the BRFS estimation, the involved computation complexity will be very high. I.e., when the sample size M is large, then the state space of timing drifts will be enlarged. Considering the fading gains, the unknown state space will become $K\times M$ dimensional, rendering a direct computation/integration infeasible. To alleviate the difficulty, particle filtering (PF) is used to implement the Bayesian inference via a simulated Monte-Carlo approach [45], relying on the sequential importance sampling (SIS).

1) PF: Using the PF, a group of discrete particles $\mathbf{x}_n^{(i)}$ with evolving probability mass (or weights) $w_n^{(i)}$ $(i=1,2,\cdots,I)$, which are simulated from a proposal density, i.e., $\mathbf{x}_n^{(i)}\sim\pi(\mathbf{x}_n^{(i)}|z_{1:n})$, are employed to approximate complex integration via numerical summation [45]. That is, the involved density $p_n(\mathbf{x}_n)$ will be computed via:

$$p_n(\mathbf{x}_n)=\sum_{i=0}^{I-1}w_n^{(i)}\times\delta(\mathbf{x}-\mathbf{x}_n^{(i)}), \tag{45}$$

where the compound state is $\mathbf{x}_n\triangleq\{M_n,\alpha_n\}$. Thus, the essence of PF is to design a proper proposal density, from which we can (1) sample I discrete particles, and (2) update the particle weights recursively. In general, given a proposal density $\pi\left(\mathbf{x}_n^{(i)}|z_{1:n}\right)$, the particle weighs $w_n^{(i)}$ are updated by:

$$w_n^{(i)}=w_{n-1}^{(i)}\times\frac{p\left(z_n|\mathbf{x}_n^{(i)}\right)\cdot p\left(\mathbf{x}_n^{(i)}|\mathbf{x}_{n-1}^{(i)}\right)}{\pi\left(\mathbf{x}_n^{(i)}|\mathbf{x}_{1:n-1},z_{1:n}\right)}. \tag{46}$$

2) Bernoulli PF: As far as Bernoulli PF (BPF) is concerned, we need to approximate the predicted spatial density via $\hat{p}_{n|n-1}(\mathbf{x})\simeq\sum_{i=0}^{I-1}w_{n|n-1}^{(i)}\times\delta\left(\mathbf{x}-\mathbf{x}_{n|n-1}^{(i)}\right)$. Given two complementary components (i.e., survival and birth), a group of discrete particles are sampled from a piece-wise distribution [26], [43], i.e.,

$$\mathbf{x}_{n|n-1}^{(i)}\sim\begin{cases}\xi_n\left(\mathbf{x}_{n|n-1}|\mathbf{x}_{n-1|n-1}^{(i)},z_{1:n-1}\right), i=1,\cdots,J, & \text{(47a)}\\ \beta_n(\mathbf{x}_{n|n-1}|z_{1:n-1}),\ i=J+1,\cdots,J+B. & \text{(47b)}\end{cases}$$

where the first J particles will approximate the survival term, whilst the later B particles are used to evaluate the birth term. Then, the associative weights evolve according to:

$$w_{n|n-1}^{(i)}=\begin{cases}\dfrac{p_s\cdot q_{n-1|n-1}}{q_{n|n-1}}\cdot\dfrac{p_n\left(\mathbf{x}_{n|n-1}^{(i)}|\mathbf{x}_{n-1|n-1}^{(i)}\right)}{\xi_n\left(\mathbf{x}_{n|n-1}|\mathbf{x}_{n-1|n-1}^{(i)},z_{1:n-1}\right)}\cdot w_{n-1|n-1}^{(i)},\\ \qquad i=1,2,\cdots,J,\\ \dfrac{p_b\times(1-q_{n-1|n-1})}{q_{n|n-1}}\times\dfrac{b_{n|n-1}\left(\mathbf{x}_{n|n-1}^{(i)}\right)}{B\times\beta_n(\mathbf{x}_{n|n-1}|z_{1:n-1})},\\ \qquad i=J+1,\cdots,J+B.\end{cases} \tag{48}$$

Usually, in order to eliminate particles with extremely small weights, a re-sample process will be adopted if necessary [46].

3) Proposal survival-density: The proposal density, related with the survival component, will be determined recursively. I.e., with the predict particles and weights of the previous time $n-2$, the posterior density of time $n-1$ will be approached after updating $J+B$ particle weights. Thus, J new particles can be simulated from the updated posterior density at time $n-1$, i.e.,

$$\begin{aligned}\mathbf{x}_{n-1|n-1}^{(i)}\sim\sum_{i=1}^{J+B}\delta\left(\mathbf{x}-\mathbf{x}_{n-1|n-2}^{(i)}\right)\times\\ \varphi_n\left(z_{n-1}|\mathbf{x}_{n-1|n-2}^{(i)}\right)\cdot w_{n-1|n-2}^{(i)},\end{aligned} \tag{49}$$

These J particles $\mathbf{x}_{n-1|n-1}^{(i)}$ $(i=1,\cdots,J)$, as survival particles, will be retained for the subsequent time n.

4) Proposal birth-density: The proposal birth density will be assigned directly as the *a priori* transitional density, i.e.,

$$\mathbf{x}_{n|n-1}^{(i)}\sim b_{n|n-1}(\alpha_n)\times b_{n|n-1}(M_n|z_{1:n-1}). \tag{50}$$

Premised on a PF approach, the predicted spatial density $p_{n|n-1}(\mathbf{x})$, which involves the $K\times M$ dimensional space, will be approximated via:

$$\begin{aligned}&\int_{\mathcal{A},\mathcal{M}}r_n(z_n|\{M_n,\alpha_n\})\cdot p_{n|n-1}(\{M_n,\alpha_n\})dM_nd\alpha_n,\\ &\simeq\sum_{i=1}^{J+B}r_n\left(z_n|\mathbf{x}_{n|n-1}^{(i)}\right)\times w_{n|n-1}^{(i)}.\end{aligned} \tag{51}$$

5) Practical Considerations: As the fading channel α_n will keep temporarily invariant within L successive slots, the observations within such a static length (in the case of $q_{n|n}>\gamma$) can be accumulated, which further improves the degree of likelihood density and thereby promotes the estimation performance. Besides, in order to reduce the population of particles when sampling from a $K\times M$ dimensional space, I particles are employed to respectively simulate fading states and timing drifts, and then I compound particles of 2-dimensional is formulated by binding them together.

An schematic flow of the proposed algorithm is summarized in **Algorithm. 1**. (1) Provided the current observation z_n, the posterior existence probability $q_{n|n}$ and the spatial density $p_{n|n}(M_n,\alpha_n)$ are estimated, by using a two-stage (prediction and update) procedure; (2) in the case of $q_{n|n}>\gamma$, the observation will be accumulated to further promote the accuracy of likelihood; (3) the unknown device as well as its associated LSI will be estimated by maximizing the posterior densities.

From the above elaboration, the involved multiplication of our proposed scheme will be measured by $O(M+I\vartheta)$.

This article has been accepted for publication in a future issue of this journal, but has not been fully edited. Content may change prior to final publication. Citation information: DOI 10.1109/TWC.2018.2796553, IEEE Transactions on Wireless Communications

(1) $O(M)$ multiplications are required when constructing the summed-energy observation. (2) In subsequent BPF, the required multiplications are basically proportional to the size of used particles I. Here, ϑ denotes the required multiplications when processing each particles, including the transitional operation and likelihood evaluation.

As demonstrated by Eq. (46) and (48), the main computation of our algorithm comes from the evaluation of Gaussian likelihood function for I independent particles $\mathbf{x}_n^{(i)}$, accompanying M power operations. We assume a configuration of M=200 and I=100, and use a single core of an *ARM Cortex A9* (which is not a cutting-edge, as far as the next-generation smartphone is concerned) to implement the involved computation. We found the algorithm will take less than 0.1 milliseconds (i.e. the real-time float-point computation). Reducing the sample size M and particle size I directly may lead to the simplified complexity, yet there involves a practical compromise between performance and complexity[1]. For the typical sensing-transmission frame length of 20∼100 milliseconds, therefore, the time-delay will be basically negligible. Also, if further considering the resource-efficient automatic generation of look-up-table [48], the power consumption is not really a big cost when implementing the algorithm locally (around 10 times per second in detection stage).

IV. NUMERICAL SIMULATIONS

In the section, the performance of the proposed algorithm will be evaluated via numerical simulations. In order to measure the detection performance, the *right detection ratio* P_D is adopted as a performance metric as in refs. [24], [35], which takes both the miss detection probability P_m and the false alarm P_f into considerations and, therefore, is more suitable to the designed Bayesian scheme.

$$P_D = 1 - p(H_1)P_m - p(H_0)P_f. \tag{52}$$

For time-dependent fading channels, the mean square error (MSE) of estimations will be evaluated, i.e.

$$\text{MSE}_\alpha \triangleq \frac{1}{N} \times \mathbb{E}\left\{\sum\nolimits_{n=1}^{N} |\hat{\alpha}_n - \alpha_n|^2/|\alpha_n|^2\right\}. \tag{53}$$

For the other important LSI, i.e. the varying timing drifts, the MSE will be calculated, i.e.

$$\text{MSE}_t \triangleq \frac{1}{N} \times \mathbb{E}\left\{\sum\nolimits_{n=1}^{N} |\hat{M}_n - M_n|^2/|M_n|^2\right\}. \tag{54}$$

In the first simulation, the representative states of fading channel are K=7 and the variance of Rayleigh fading is $\sigma_\alpha^2 = 0.5$; the static length is L=20. The sample size is M=100. The birth probability is p_b=0.8 and the survival probability is p_s=0.2. The total particle size is I =200, i.e. $J = B = 100$. We find from Fig. 3 (a)-*Left*, in the case of correlated transmission intervals (i.e., *Type-1*), the dynamical timing drifts will be varied in a correlated manner, as in Eq. (15). Using the proposed scheme, the unknown drift can be effectively tracked. From the MSE performance in Fig. (a)-*Right*, the estimation of unknown timing is accurate relatively. Relying on the numerical results, the estimation error, i.e. $\hat{M}_n - M_n$, will be distributed basically according to one Laplace density, i.e. $\mathscr{L}(0, 3.3)$. Despite the maximum deviation of $M/2$ (i.e. $|M_n| \leq$50 when M=100), the estimation error will never excess 15, and the mean MSE is only about 3.076 when SNR is 14dB. In Fig. 3-(b), the same observation will be made to the uncorrelated transmission intervals (i.e. *Type-2*), yet with the increased estimation errors, due to the completely random timing drifts (see Fig. 3-(b)-*Left*).

Algorithm 1 Asynchronous device detections for C-D2D

Input: Observation $z_{1:n},\ n = 1, \cdots, N-1$,
Initial density $q_{1|1},\ p_{1|1}(\{M_1, \alpha_1\})$,
Feasible fading state $\mathcal{A}$ and its TPM $\mathbf{\Pi}_{K\times K}$,
Feasible timing transitional model $M_n = T(M_{n-1})$.
Output: Posterior densities $q_{n|n},\ p_{n|n}(\{M_n, \alpha_n\})$,
Existence state s_n and LSI, i.e. $\{M_n, \alpha_n\}$.

⋆ Initialize the particles $\left\{\mathbf{x}_1^{(i)}, w_1^{(i)}\right\}$, $I = 1, \cdots, J+B$.
for $n \to 1$ to N **do**
⋆ Calculate the predicted density $q_{n|n-1}$ via Eq. (34).
⋆ Simulate $(J+B)$ particles $\mathbf{x}_{n|n-1}^{(i)}$ from Eq. (47).
⋆ Calculate the predicted particle weights $w_{n|n-1}^{(i)}$, and then normalize such particle weights.
⋆ Evaluate the likelihood density $\varphi_n(z_n|\{M_n, \alpha_n\}, s_n)$.
⋆ Update the particles and their weights, and obtain $\{\mathbf{x}_{n|n}^{(i)}, w_{n|n}^{(i)}\}$.
⋆ Calculate the existence density $\hat{q}_{n|n}$ via Eq. (36), and estimate the active state $\hat{s}_n$ via Eq. (39).
⋆ Approximate the spatial density $\hat{p}_{n|n}(\{M_n, \alpha_n\})$ via Eqs. (35) and (51), and estimate unknown LSI $\{M_n, \alpha_n\}$ via Eq. (40).
if $\hat{q}_{n|n} > \gamma$ and $\text{mod}(n, L) > 0$ **then**
◇ Accumulate the observations in $[\lfloor n/L \rfloor \times L + 1, n]$;
◇ Re-calculate the likelihood using the accumulated observations, and re-estimate fading state $\hat{\alpha}_n$.
end if
⋆ Output the estimated state $\hat{s}_n$ and the related LSI $\{\hat{M}_n, \hat{\alpha}_n\}$.
end for

A. Correlated timing drifts

We now focus on the estimation performance in the presence of correlated timing drifts. As noted from Fig. 4, the sample size M will affect the estimation MSE. To be specific, a large sample size M will lead to the increased estimation accuracy. A rough detection gain of 2dB will be attained by a smaller sample M=100, compared with the case of M=200. This is because we consider the *worst* situation in our analysis, where the maximum deviation samples is proportional to the sample size M, i.e. $\max(|M_n|) = M/2$. Therefore, the larger the

[1]For the sample size M, the tradeoff between sensing accuracy and transmission throughput has been investigated by Liang et.al. [47]. Here, we only refer to a compromise between detection accuracy and complexity computation. Notice that, for the concerned device detection with unknown timing drift, a larger sample size M was supposed to increase the accuracy of likelihood density and the detection performance. As shown by subsequent analysis, the increased uncertainty in timing drift, i.e. $M_n \in [-M/2, M/2]$, would degrade the detection. So, there involves another interesting compromise in configuring M.

This article has been accepted for publication in a future issue of this journal, but has not been fully edited. Content may change prior to final publication. Citation information: DOI 10.1109/TWC.2018.2796553, IEEE Transactions on Wireless Communications

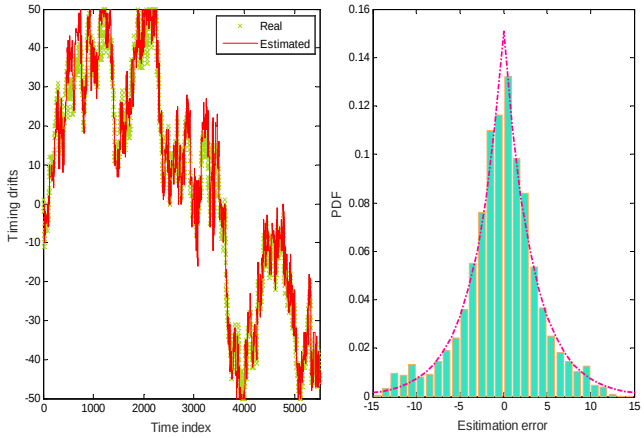

(a)

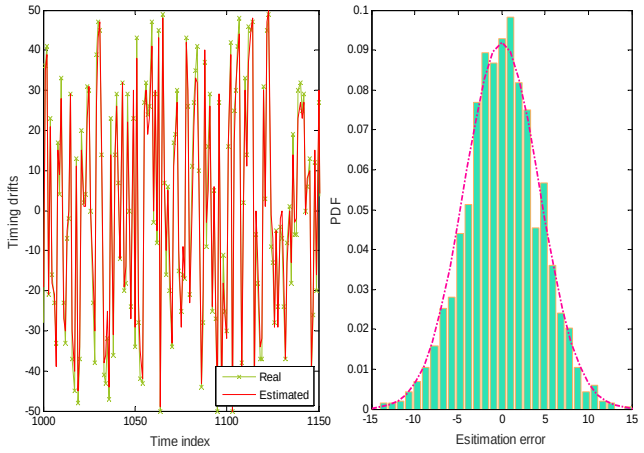

(b)

Fig. 3. (a)-*Left*: The estimation performance of dynamical timing drifts in the context of correlated emission intervals. (a)-*Right* The estimation errors of timing drifts. In the simulation, the maximum timing drift is M=100, and the SNR is configured to 12dB. The estimation errors may follow a Laplace distribution $\mathscr{L}(0, 3.3)$. (b)-*Left* The estimation performance of dynamic timing drift in the context of correlated emission intervals. (b)-*Right* The estimation error of the timing drifts, which follows a Gaussian distribution $\mathscr{N}(0, 4.3^2)$.

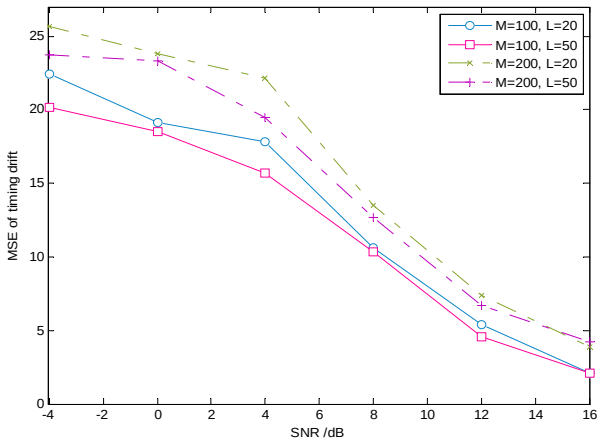

Fig. 4. MSE performance of dynamic timing drifts in the context of correlated transmission intervals.

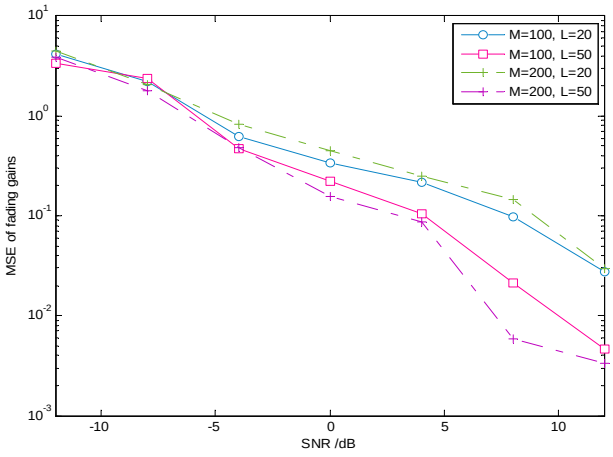

Fig. 5. MSE performance of time-dependent fading channels in the context of correlated transmission intervals.

sample size M, the larger the uncertainty of varying timing is. Besides, given the sample size M, the estimation performance will be improved by an increased static length L.

The tracking performance of varying fading gains is shown in Fig. 5. We can see that, with the increasing of a static fading length L, the MSE performance of various sample sizes (both M=100 and M=200) will be promoted significantly. This is easy to follow. The larger the static length L, the more observations (within a static length) will be accumulated, resulting in the more accurate likelihood information. However, it is noted that, when the sample size is M=200, the MSE of estimated fading gain will be slightly inferior to that of M=100 (when $L = 20$). Despite more samples of M=200 and the increased accuracy of likelihood, the maximum timing deviations will also be increased to 100 (e.g. from 50 in the case of M=100). As a consequence, the improved likelihood density would be compromised by the increased timing uncertainty. The theoretical analysis on proper configuration of sample size M remains still an open issue for future studies.

The detection probability is given by Fig. 6. First, we can see that increasing the static fading length L can enhance the accuracy of device detection, in the presence of unknown timing and channel fading. Taking a sample size M=200 for example, a rough gain of 5dB will be attained if L=50, compared to another case of L=20. In contrast to a common sense, for a small static fading length (e.g. L=20), increasing the sample size M *cannot* always achieve the detection gains, in the situation of asynchronous D2D device detection. As mentioned, only the improvement on the likelihood accuracy surpasses the enlargement of timing uncertainty, can the detection performance be improved, as the case of large static length L=50.

B. Uncorrelated timing drifts

Next, we will study the estimation/detection performance with uncorrelated timing drifts. It is seen from Fig. 7 that, with the completely random timing drifts, the estimation MSE will converge to a stable value, after the SNR surpassing 12dB. For example, when M =100 and L=50 the mean MSE will be

This article has been accepted for publication in a future issue of this journal, but has not been fully edited. Content may change prior to final publication. Citation information: DOI 10.1109/TWC.2018.2796553, IEEE Transactions on Wireless Communications

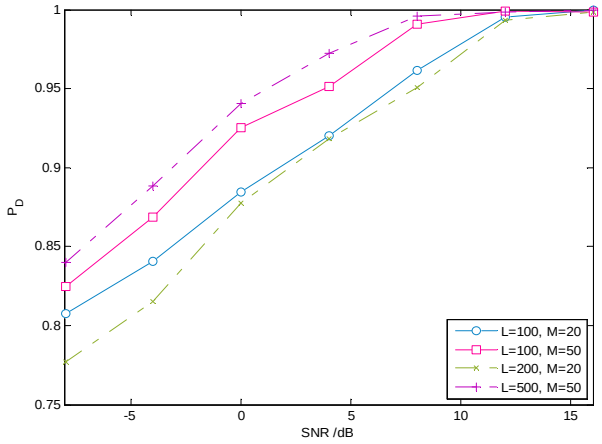

Fig. 6. Device detection performance in the context of correlated transmission intervals.

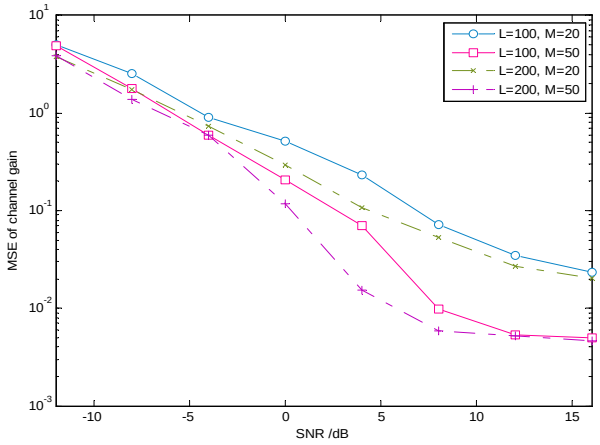

Fig. 8. MSE performance of time-dependent fading channels in the context of uncorrelated transmission intervals.

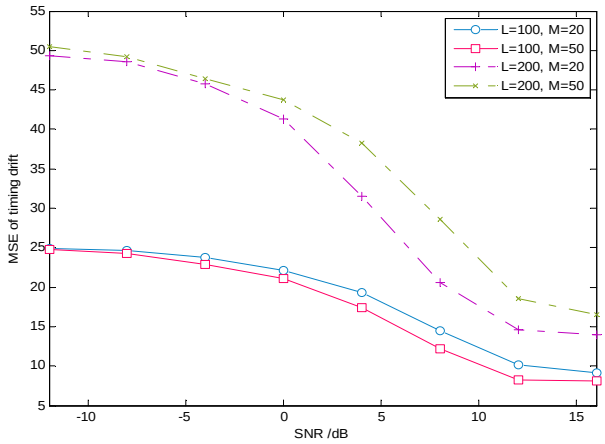

Fig. 7. MSE performance of dynamic timing drifts in the context of uncorrelated transmission intervals.

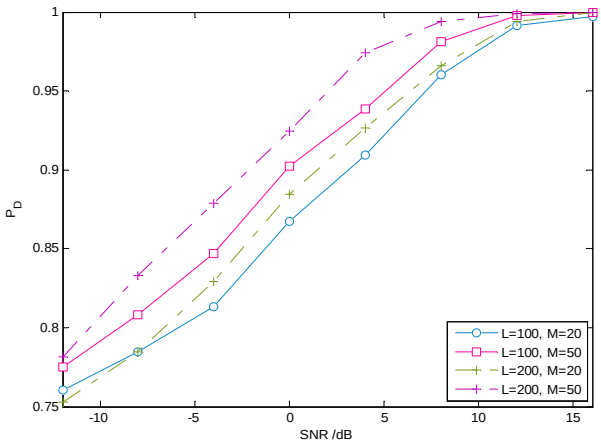

Fig. 9. Device detection performance in the context of uncorrelated transmission intervals.

8.25 (samples) in high SNR regions (e.g. SNR>10dB). This is relatively different from the numerical results of correlated timing drifts. Meanwhile, we find that the estimation MSE of uncorrelated timing drifts will be higher than that of correlated drifts. Taking M=100 and L=50 for example, the mean MSE for uncorrelated drifts is about 8.22 samples when SNR=16dB, while the mean MSE under correlated drifts will only be 2.16 samples. This is mainly attributed to the underlying dynamics of correlated drifts, which may be further utilized to improve the estimation performance.

When it comes to varying fading channels, the estimation accuracy will be comparable to that of the correlated timing drifts. In the high SNR region, the slightly more accurate estimation will be obtained in the case of correlated timing drifts. Taking SNR=12dB for example, the MSE of uncorrelated drifts is about 0.005 when M=200 and L=50. While for the correlated drifts, the MSE becomes 0.0045.

The performance of device detection under uncorrelated timing drifts are shown by Fig. 9. Taking M=200 and L=50, when SNR is larger than 12dB, the right detection probability will be 1. We will see that, in this case, the residual errors of unknown timing drift is about 15 samples, while the relative error of fading channels will be 0.005. By effectively suppressing the involved information uncertainties, the proposed scheme is applicable to asynchronous D2D device detection, even with varying fading gain and unknown timing drifts.

C. Comparative analysis

We firstly compare the detection performance of different timing drifts. In the simulations, the static length is L=20 and the sample size is M=100. As expected, the detection accuracy in the context of correlated timing drifts will be relatively superior to that of uncorrelated drifts. Notice from Fig. 10-a that, in high SNRs region (e.g. SNR>8dB), the detection performance of two different timing drifts will be comparable.

Although the aforementioned fixed-threshold technique would be feasible, here we focus on the comparison of another method in the scenario of asynchronous detection, which, to even things up, is similarly based on a Bayesian rule (rather than another Neyman-Pearson criterion) by exploiting the available partial statistic information. Since there is no coordination from BS, we have to assume that only limited information on both unknown timing drift and fading gain

This article has been accepted for publication in a future issue of this journal, but has not been fully edited. Content may change prior to final publication. Citation information: DOI 10.1109/TWC.2018.2796553, IEEE Transactions on Wireless Communications

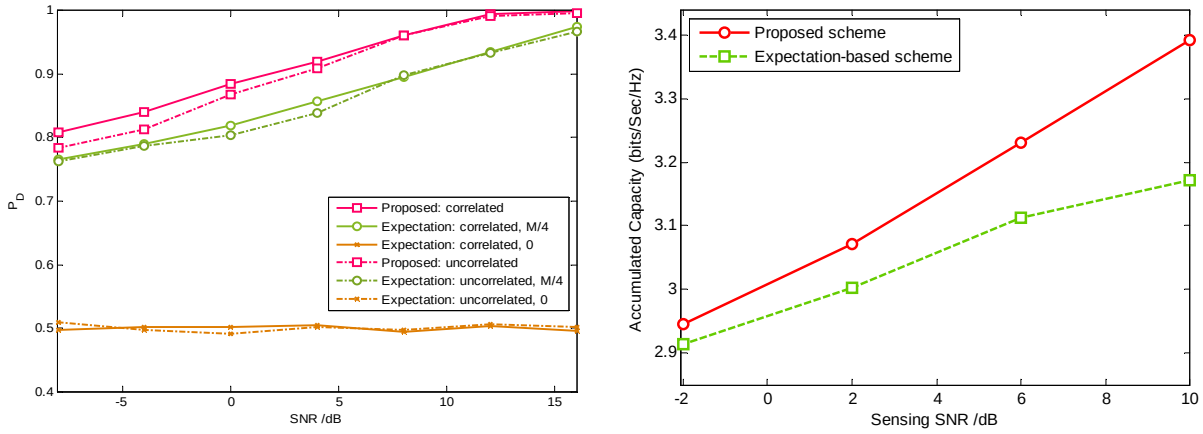

(a) (b)

Fig. 10. (a) Device detection performance of the designed scheme vs the expectation likelihood-based methods. (b) The accumulated capacity for shared accessing scenario of different detection schemes.

can be available. In this case, the likelihood-based technique can be utilized. To be specific, when the conditional likelihood $p(z_n|s_n = 1, \mathbb{E}_{\mathcal{M}}\{M_n\}, \mathbb{E}_{\mathcal{A}}\{\alpha_n\})$ is larger than $p(z_n|s_n = 0)$, we will have $\hat{s}_n$=1, and otherwise, $\hat{s}_n$=0. Since the timing drifts M_n will be distributed in $[-M/2, M/2]$, one simple and direct solution is to assume $\mathbb{E}_{\mathcal{M}}\{M_n\} = 0$. I.e., the detector will be totally *unconscious* of real-time drifts. From the simulation result, with the two-level information uncertainty aroused by varying fading and the timing drifts, the detection performance will be significantly deteriorated. For example, the right detection probability P_D will be 0.5, no matter what the SNR is. Similar results can be observed when the uncorrelated drifts are concerned.

In fact, more partial statistic information (i.e. expectation) on unknown timing drifts can be further exploited. For example, we note from simulation results that, when the *expectation* on timing deviations is configured to a half of the sample size (or maximum deviation), i.e. $\mathbb{E}_{\mathcal{M}}\{M_n\} = M/4$, the detection performance of likelihood-based methods will be improved, compared with the simple assumption $\mathbb{E}_{\mathcal{M}}\{M_n\} = 0$. Even so, the partial information inspired detection scheme still achieves the less attractive performance, as in Fig. 10-a. In comparison, by tracking two unknown LSI and suppressing the information uncertainty, a rough gain about 5∼6dB can be obtained by our new scheme.

Finally, we investigated the accumulated capacity in shared access scenarios. We consider two local links, one conducts primary transmissions and the other one (i.e. secondary link) manages to share the spectrum via a listen-before-talk strategy. Due to the false detection (with the probability $p(H_1|H_0)$), the capacity of primary user will be degraded. The missed detection (with the probability $p(H_0|H_1)$), on the other hand, will affect the shared capacity of secondary transmissions. Without losing generality, we assume the normalized capacity of primary user with no interference from shared transmission is C_p, and the capacity when the missed detection occurs will be decreased to C'_p. The shared capacity of secondary user (i.e. conducting proximity-based transmission) is C_s. It is easily found the accumulated capacity is:

$$\begin{aligned} C_a =& C_p \cdot p(H_1|H_1)p(H_1) + C'_p \cdot [1 - p(H_1|H_1)]p(H_1) \\ &+ C_s \cdot [1 - P(H_1|H_0)]p(H_0). \end{aligned}$$

We then evaluated the promotion of accumulated capacity C_a by our proposed scheme. In numerical analysis, we configured $L = 20$, $M = 100$, $\mathbb{E}_{\mathcal{M}}\{M_n\} = M/4$, $p(H_1)$=$p(H_0)$=0.5, C_p=2.32 bit/sec/Hz (i.e. SNR_P=4), C'_p=1.32 bit/sec/Hz (i.e. $SINR_P$=1.5), and C_s=4.39 bit/sec/Hz (i.e. SNR_S=20). From Fig. 10-b, we noted the proposed scheme can enhance the accumulated capacity C_a of shared accessing. Taking the sensing SNR of 10dB for example, the accumulated capacity can be improved by 7% by using the new scheme, compared with a classical detection method (i.e. the likelihood-based detection utilizing the expectation of unknown LSI.)

More importantly, except for promoting the detection performance, the acquired LSI will be also of great significance, for example, to underlay D2D communications [49]. To be specific, the accurate fading gain will provide additional information for subsequent D2D mode selection and resource allocations. For example, consider two primary devices talk with each other via the time division duplexing (TDD) scheme, then the probed channel gain permits the real-time power adaption of shared transmission to limit its interference (e.g. with either peak or averaging interference constraint). As a result, the uninterrupted transmission of shared user and the harmonious coexistence between primary and secondary links would become a reality. To this end, the additional shared capacity can be also achieved, with the aid of our proposed scheme and the acquired channel information. Such additional benefits would be covered in our future studies.

V. Conclusions

In this work, we focus on the device discovery/detection of asynchronous cognitive device-to-device communications. Due to the distributed asynchronous nature of the system, the task is greatly complicated by unknown timing drifts and

fading channels. In order to achieve the reliable detection, we design a novel deep sensing paradigm to combat destructive effects from unknown LSI. The underlying dynamics of two unknown states are fully concerned, and a sequential Bayesian scheme is proposed, which acquires the varying timing drifts and fading channels when directly performing device detection. To solve the complex MED problem, the two-stage recursive estimation is implemented, and the PF-based numerical approximation is further used to alleviate the computation complexity. Two types of timing drifts are considered, and the detection/estimation performance are numerically evaluated. It is demonstrated that, by dynamically tracking unknown drifts and fading gains, the detection performance will be improved significantly, compared to the expectation-based likelihood method. Our new scheme may further provide the useful information for transmission optimisation, e.g. the mode selection based on fading gains. By increasing the configuration flexibility, this scheme will be of promise to the emerging D2D communications, especially in adverse environments, e.g., out-of-coverage or publicity safety scenarios.

ACKNOWLEDGMENT

We greatly thank anonymous reviewers for their constructive comments and helpful feedback that allowed us to improve the paper significantly. We would also like to express our heartfelt thanks to Dr. Fahmy Suhaib of the University of Warwick, for his kind help in the hardware evaluation of the algorithm.

REFERENCES

[1] L. Zhang, M. Xiao, G. Wu, M. Alam, Y.-C. Liang and S. Li, "A Survey of Advanced Techniques for Spectrum Sharing in 5G Networks," *IEEE Wireless Communications*, vol. 24, no. 5, pp. 44-51, Oct. 2017.

[2] X. Lin, J. G. Andrews, A. Ghosh, and R Ratasuk, "An overview of 3GPP device-to-device proximity services," *IEEE Communications Magazine*, vol. 52, no. 4, pp. 40-48, 2014.

[3] J. Seppala, T. Koskela, T. Chen, and S. Hakola, "Network controlled Device-to-Device (D2D) and cluster multicast concept for LTE and LTE-A networks," in Proc. of *IEEE Wireless Communications and Networking Conference (WCNC)*, pp. 986-991, March 2011.

[4] M. J. Yang, S. Y. Lim, H. J. Park, and N. H. Park, "Solving the data overload: Device-to-device bearer control architecture for cellular data offloading," *IEEE Vehicular Technology Magazine*, vol. 8, no. 1, pp. 31-39, 2013.

[5] L. Lei, Y. Kuang, X. (Sherman) Shen, C. Lin, and Z. Zhong, "Resource Control in Network Assisted Device-to-Device Communications: Solutions and Challenges," *IEEE Communication Magazine*, vol. 52, no. 6, pp. 108-117, Jun. 2014.

[6] Cisco Visual Networking Index, *Global Mobile Data Traffic Forecast Update 2012-2017*, White Paper, http//www.cisco.com/en/US/solutions/collateral/ns341/ns525/ns537/ns705/ns827/ whitepaperc11-520862.html, 6th, 2013 Feb.

[7] X. M. Shen, "Device-to-device communication in 5G cellular networks," *IEEE Network*, vol. 29, no. 2, pp.2-3, 2015.

[8] C. Q. Fan, B. Li, C. L. Zhao, W. S. Guo, and Y.-C. Liang, "Learning-based Spectrum Sharing and Spatial Reuse in mm-Wave Ultra Dense Networks," *IEEE Transactions on Vehicular Technology,* 2017, DOI: 10.1109/TVT.2017.2750801.

[9] Y. Peng, Q. Gao, S. Sun, and Y. Zheng, "Discovery of device-device proximity: Physical layer design for D2D discovery," in Proc. of *IEEE/CIC International Conference on Communications in China-Workshops (CIC/ICCC)*, pp. 176-181, 2013.

[10] A. Asadi, Q. Wang, and V. Mancuso, "A survey on device-to-device communication in cellular networks," *IEEE Communications Surveys & Tutorials*, vol. 16, no. 4, pp.1801-1819, 2014.

[11] G. Fodor, E. Dahlman, and G. Mildh, "Design aspects of network assisted device-to-device communications," *IEEE Communications Magazine*, vol. 50, no. 3, pp.170-177, 2012.

[12] E. Yaacoub and O. Kubbar, "Energy-efficient device-to-device communications in LTE public safety networks," in Proc. of *IEEE Global Communications Conference (Globecom Workshops)*, pp.391-395, 2012.

[13] G. Fodor, S. Parkvall, S. Sorrentino, et.al. "Device-to-device communications for national security and public safety," *IEEE Access*, vol. 2, pp.1510-1520, 2014.

[14] B. Kaufman, J. Lilleberg, and B. Aazhang. "Spectrum Sharing Scheme Between Cellular Users and Ad-hoc Device-to-Device Users," *IEEE Transactions on Wireless Communications*, vol. 12, no. 3, pp. 1038-1049, March 2013.

[15] C. Xu, L. Song, Z. Han, Q. Zhao, X. Wang, and B. Jiao, "Interference-aware resource allocation for device-to-device communications as an underlay using sequential second price auction," in Proc. of *IEEE International Conference on Communications (ICC)*, pp. 445-449, June 2012.

[16] J. Ma, G. Y. Li, and B. H. Juang, "Signal Processing in Cognitive Radio," *The Proceedings of IEEE*, vol. 97, no. 5, May 2009, pp. 805-823.

[17] E. Axell, G. Leus, E. G. Larsson, and H. V. Poor, "Spectrum Sensing for Cognitive Radio: State-of-the-art and recent advances," *IEEE Signal Processing Magazine*, vol. 29, no. 3, May 2012, pp. 101-116.

[18] H. Tang, Z. Ding, and B. C. Levy, "Enabling D2D communications through neighbor discovery in LTE cellular networks," *IEEE Transactions on Signal Processing*, vol. 62, no. 19, pp. 5157-5170, October 2014.

[19] 3GPP "3rd generation partnership project technical specification group SA study on architecture enhancements to support proximity services (ProSe) (Release12)," TR#23.703#V0.4.1, June 2013.

[20] N. Wang and T. A. Gulliver, "Low-Complexity Census-Based Collaborative Compressed Spectrum Sensing for Cognitive D2D Communications," in Proc. of *2015 IEEE Global Communications Conference (GLOBECOM)*, 6-10th Dec. 2015, pp. 1-7.

[21] Y.-C. Liang, K. C. Chen, G. Y. Li, and P. Mähönen, "Cognitive radio networking and communications: an overview," *IEEE Transactions on Vehicular Technology,* vol. 60, no. 7, September 2014, pp. 3386-3407.

[22] F. F. Digham, M. S. Alouini, and M. K. Simon, "On the Energy Detection of Unknown Signals Over Fading Channels," in Proc. of *IEEE international Conference on Communications (ICC)*, Anchorage, AK, May 2003, vol. 5, pp. 3575-3579.

[23] Y. H. Zeng and Y.-C. Liang, "Eigenvalue-based Spectrum Sensing Algorithms for Cognitive Radio," *IEEE Trans Commun.*, vol. 57, 2009, pp. 1784-1793.

[24] B. Li, C. L. Zhao, M. W. Sun, Z. Zhou, and A. Nallanathan, "Spectrum Sensing for Cognitive Radios in Time-Variant Flat Fading Channels: A Joint Estimation Approach," *IEEE Transactions on Communications*, 2014, vol. 62, no. 8, pp. 2665-2680.

[25] B. Li, M. W. Sun, X. F. Li, A. Nallanathan, C. L. Zhao, "Energy Detection based Spectrum Sensing for Cognitive Radios Over Time-Frequency Doubly Selective Fading Channels," *IEEE Transactions on Signal Processing,* vol. 63, no. 2, Jan. 2015, pp. 402-417.

[26] B. Li, S. H. Li, A. Nallanathan, and C. L. Zhao, "Deep Sensing for Future Spectrum and Location Awareness 5G Communications," *IEEE Journal Selected Areas Communications*, vol. 33, no. 7, 2015, pp. 1331-1344.

[27] B. Ristic and A. Farina, "Target tracking via multi-static Doppler shifts," *IET Proc. Radar, Sonar Navig.*, vol. 7, no. 5, 2013, pp. 508-516.

[28] B.-T. Vo, D. Clark, B.-N. Vo, and B. Ristic, "Bernoulli forward-backward smoothing for joint detection and tracking," *IEEE Trans. Signal Processing*, vol. 59, No. 9, 2011, pp. 4473-4477.

[29] S. Tekinalpl and A. A. Alatan, "Efficient Bayesian Track-Before-Detect," in Proc. of 2006 International Conference on Image Processing (ICIP), 2006, pp. 2793-2796.

[30] R. Mahler, *Statistical Multisource Multitarget Information Fusion*. Norwood, MA, USA: Artech House, 2007.

[31] B.-T. Vo and B.-N. Vo, "A Random Finite Set Conjugate Prior and Application to Multi-target Tracking," in Proc.*7th IEEE Int. Conf. Intell. Sens., Sens. Netw. Inf. Proc. (ISSNIP)*, Adelaide, Australia, Dec. 2011, pp. 431-436.

[32] M. Jung, K. Hwang, and S. Choi, "Joint mode selection and power allocation scheme for power-efficient device-to-device (D2D) communication," in Proc. of *IEEE Vehicular Technology Conference (VTC-Spring)*, pp. 1-5, 2012.

[33] J. Seppala , T. Koskela , T. Chen and S. Hakola, "Network controlled Device-to-Device (D2D) and cluster multicast concept for LTE and LTE-A networks," in Proc. of *IEEE Wireless Communications & Networking Conference (WCNC)*, pp. 986-991, 2011.

[34] B. Vujitic, N Cackov, and S. Vujitic. "Modeling and characterization of traffic in public safety wireless network," in Proc. of *Int. Symp.*

Performance Evaluation of Computer and Telecommunication Systems, Edinburgh, UK, July 2005, pp. 213-223.

[35] B. Li, S. H. Li, Y. J. Nan, A. Nallanathan, C. L. Zhao, and Z. Zhou, "Deep Sensing for Next-generation Dynamic Spectrum Sharing: More Than Detecting the Occupancy State of Primary Spectrum," *IEEE Transactions on Communications,* vol. 63, no. 7, 2015, pp. 2442-2457.

[36] P. Sadeghi, R. Kennedy, P. Rapajic, and R. Shams, "Finite-state Markov Modeling of Fading Channels: A Survey of Principles and Applications," *IEEE Signal Processing Magazine*, vol. 25, no. 5, 2008, pp. 57-80.

[37] H. S. Wang and N. Moayeri, "Finite-state Markov Channel: A Useful Model for Radio Communication Channels," *IEEE Transactions on Vehicular Technology,* vol. 44, no. 1, Feb. 1995, pp. 163-171.

[38] H. S. Wang and P. Chang, "On Verifying the First Order Markovian Assumption for A Rayleigh Fading Channel Model," *IEEE Transactions on Vehicular Technology,* vol. 45, no. 2, May 1996, pp. 353-357.

[39] W. B. Davenport Jr. and W. L. Root, *An Introduction to the Theory of Random Signals and Noise,* New York : IEEE Press, 1958.

[40] S. J. Miller and M. J. Nigrini. "The modulo 1 central limit theorem and Benford's law for products," *arXiv preprint math/0607686,* 2006.

[41] P. Pedrosa, R. Dinis, F. Nunes, et al. "Phase Drift Estimation and Symbol Detection in Digital Communications: A Stochastic Recursive Filtering Approach," *IEEE Communications Letters,* 2012, vol. 16, no. 16, pp.854-857.

[42] B.-T. Vo, B.-N. Vo, and A. Cantoni, "Bayesian filtering with random finite set observations," *IEEE Trans. Signal Process.*, vol. 56, no. 4, pp. 1313-1326, 2008.

[43] B. Ristic, B.-T. Vo, B.-N. Vo, and A. Farina, "A Tutorial on Bernoulli Filters: Theory, Implementation and Applications," *IEEE Trans. Signal Process.*, vol. 61, no. 13, July, 2013, pp. 3406-3430.

[44] Z. Chen, "Bayesian Filtering: From Kalman Filters to Particle Filters, and Beyond," *Statistics*, 2003.

[45] P. M. Djuric, J. H. Kotecha, J. Q Zhang, Y. F. Huang, T. Ghirmai, M. F. Bugallo, and J. Miguez, "Particle filtering," *IEEE Signal Processing Magazine*, vol. 20, no. 5, 2003, pp. 19-38.

[46] A. Doucet, S. Godsill, and C. Andrieu, "On sequential Monte Carlo sampling methods for Bayesian filtering," *Statistics and computing*, 2000, vol. 10, no. 3, pp. 197-208.

[47] Y. C. Liang, Y. H. Zeng, E. C. Y. Peh, and A.T. Hoang, "Sensing-Throughput Tradeoff for Cognitive Radio Networks," *IEEE Transactions on Wireless Communications,* vol. 7, no. 4, 2008, pp. 1326-1337.

[48] L. Deng, C. Chakrabarti, N. Pitsianis, et al. "Automated optimization of look-up table implementation for function evaluation on FPGAs," in *Proc of SPIE*, 2015, 7444, pp. 744413-744413-9.

[49] L. Wang, H. Tang, H. Wu, et al. "Resource Allocation for D2D Communications Underlay in Rayleigh Fading Channels," *IEEE Transactions on Vehicular Technology*, vol. 66, no. 2, 2017, pp. 1159-1170.